Enhancer of zeste homolog 2 (EZH2) regulates adipocyte lipid metabolism independent of adipogenic differentiation: Role of apolipoprotein E

Received for publication, November 27, 2018, and in revised form, March 25, 2019 Published, Papers in Press, April 10, 2019, DOI 10.1074/jbc.RA118.006871

Nicole K. H. Yiew[‡§1], Charlotte Greenway[§], Abdalrahman Zarzour[§¶], Samah Ahmadieh[§¶], Brandee Goo[§¶], David Kim[§], Tyler W. Benson[§], Mourad Ogbi[§], Yao Liang Tang[§¶], Weiqin Chen[‖], David Stepp[§‖], Vijay Patel[**], Renee Hilton[‡‡], Xin-Yun Lu[§§], David Y. Hui[¶¶], Ha Won Kim[§¶], and Neal L. Weintraub[§¶2]

From the Departments of [‡]Pharmacology and Toxicology, [¶]Medicine (Division of Cardiology), [‖]Physiology, [§§]Neuroscience and Regenerative Medicine, [**]Cardiothoracic and Vascular Surgery, and [‡‡]Minimally Invasive and Digestive Diseases Surgery and the [§]Vascular Biology Center, Medical College of Georgia at Augusta University, Augusta, Georgia 30912 and the [¶¶]Department of Pathology and Laboratory Medicine, University of Cincinnati, Cincinnati, Ohio 45267

Edited by Jeffrey E. Pessin

Enhancer of zeste homolog 2 (EZH2), an epigenetic regulator that plays a key role in cell differentiation and oncogenesis, was reported to promote adipogenic differentiation *in vitro* by catalyzing trimethylation of histone 3 lysine 27. However, inhibition of EZH2 induced lipid accumulation in certain cancer and hepatocyte cell lines. To address this discrepancy, we investigated the role of EZH2 in adipogenic differentiation and lipid metabolism using primary human and mouse preadipocytes and adipose-specific EZH2 knockout (KO) mice. We found that the EZH2-selective inhibitor GSK126 induced lipid accumulation in human adipocytes, without altering adipocyte differentiation marker gene expression. Moreover, adipocyte-specific EZH2 KO mice, generated by crossing EZH2 floxed mice with adiponectin-Cre mice, displayed significantly increased body weight, adipose tissue mass, and adipocyte cell size and reduced very low-density lipoprotein (VLDL) levels, as compared with littermate controls. These phenotypic alterations could not be explained by differences in feeding behavior, locomotor activity, metabolic energy expenditure, or adipose lipolysis. In addition, human adipocytes treated with either GSK126 or vehicle exhibited comparable rates of glucose-stimulated triglyceride accumulation and fatty acid uptake. Mechanistically, lipid accumulation induced by GSK126 in adipocytes was lipoprotein-dependent, and EZH2 inhibition or gene deletion promoted lipoprotein-dependent lipid uptake *in vitro* concomitant with up-regulated apolipoprotein E (*ApoE*) gene expression. Deletion of *ApoE* blocked the effects of GSK126 to promote lipoprotein-dependent lipid uptake in murine adipocytes. Collectively, these results indicate that EZH2 inhibition promotes lipoprotein-dependent lipid accumulation via inducing *ApoE* expression in adipocytes, suggesting a novel mechanism of lipid regulation by EZH2.

Adipogenic differentiation is a complex process that involves the coordinated interplay of epigenetic and transcriptional mechanisms, leading to induction of key adipogenic genes (*i.e.* peroxisome proliferator-activated receptor γ (PPARγ)[3] and adiponectin) and the accumulation of intracellular lipid droplets, the pathognomonic feature of mature adipocytes. Adipocyte lipid content is, in turn, governed by the balance between anabolic and catabolic reactions (1), including fatty acid (FA) uptake/esterification, *de novo* lipogenesis (DNL), and cytosolic lipolysis. Adipocyte triglycerides can also be derived from triglyceride-rich lipoproteins, including very low-density lipoprotein (VLDL) and chylomicrons. These lipoprotein-dependent processes are in part mediated by apolipoprotein E (*ApoE*) (2), which is highly expressed in adipocytes and modulates lipoprotein-dependent metabolism (2–4). Whereas epigenetic regulation of adipogenic differentiation has been extensively studied, little is known about mechanisms of epigenetic regulation of adipocyte lipid metabolism *per se*.

Among the epigenetic regulators that have been reported to regulate adipogenic differentiation is enhancer of zeste homolog 2 (EZH2), a histone methyltransferase enzyme. EZH2, the catalytic subunit of the core polycomb repressive complex 2 (PRC2), carries out cellular histone H3 lysine 27 di/trimethylation (H3K27me$^{2/3}$), which is commonly associated with silenc-

This work was funded by National Institutes of Health Grants HL124097, HL126949, and HL134354 (to N. L. W.) and AR070029 (to Y. L. T. and N. L. W.) and an American Heart Association Predoctoral Fellowship Award (to N. K. H. Y). The authors declare that they have no conflicts of interest with the contents of this article. The content is solely the responsibility of the authors and does not necessarily represent the official views of the National Institutes of Health.

This article contains Figs. S1–S6.

[1] Present address: Dept. of Pathology and Immunology, Washington University School of Medicine, St. Louis, MO 63110.

[2] To whom correspondence should be addressed: Dept. of Medicine, Division of Cardiology, Vascular Biology Center, Medical College of Georgia at Augusta University, 1460 Laney Walker Blvd., Augusta, GA 30912. Tel.: 706-721-4584; Fax: 706-721-9799; E-mail: nweintraub@augusta.edu.

[3] The abbreviations used are: PPAR, peroxisome proliferator-activated receptor; EZH2, enhancer of zeste homolog 2; H3K27, histone 3 lysine 27; me^2 and me^3, dimethylation and trimethylation, respectively; Adipoq, adiponectin; VLDL, very low-density lipoprotein; *ApoE*, apolipoprotein E; ApoB-100, apolipoprotein B-100; FA, fatty acid; DNL, *de novo* lipogenesis; PRC2, polycomb repressive complex 2; SQ, subcutaneous; SV, stromal vascular; ORO, Oil Red O; IBMX, 3-isobutyl-1-methylxanthine; DiI, 1,1′-dioctadecyl- 3,3,3′,3′-tetramethylindocarbocyanine perchlorate; IDL, intermediate-density lipoprotein; LDL, low-density lipoprotein; HDL, high-density lipoprotein; DZNEP (3-deazaneplanocin A); KO, knockout; LPL, lipoprotein lipase; MSC, mesenchymal stem cell; ddH_2O, double-distilled H_2O; DMEM, Dulbecco's modified Eagle's medium; MA, mature adipocytes.

ing of differentiation genes. Notably, Wang *et al.* (5) demonstrated that EZH2-induced H3K27me^3 of Wnt gene promoters facilitated adipogenic differentiation of murine preadipocytes. Likewise, Yi *et al.* (6) showed that S6K1-induced EZH2 recruitment catalyzed H3K27me^3 and promoted adipogenesis in murine cell lines. However, the majority of data implicating a role for EZH2 in promoting adipogenic differentiation were obtained in murine cells (5–9). Notably, epigenetic mechanisms that control cell differentiation and lipid metabolism can differ in a species– and cell type–specific manner.

EZH2 is overexpressed in various tumor cell types, including prostate and breast cancer, and blocking EZH2 activity by pharmacological inhibitors has emerged as a key epigenetic strategy for cancer therapeutics that is currently under investigation in clinical trials (10–13). Interestingly, several studies have reported accumulation of cytoplasmic lipid droplets in human breast cancer cells and hepatocytes in response to an EZH2 inhibitor (3-deazaneplanocin A (DZNEP)) (14, 15), but whether this represents a cell- and/or species-dependent effect is unknown. Thus, it is imperative to perform studies in primary human adipocytes and *in vivo* mouse models to determine the potential impact of EZH2 inhibition on adipose tissue biology.

Here, we investigated the role of EZH2 in adipogenic differentiation and lipid metabolism using primary human and mouse preadipocytes and adipocyte-specific EZH2 knockout (KO) mice. We demonstrate that pharmacological inhibition of EZH2 in human adipocytes and adipocyte-specific EZH2 deletion in mice promote adipocyte lipid accumulation. Mechanistically, EZH2 inhibition or gene deletion up-regulates *ApoE* expression, which in turn promotes lipoprotein-dependent lipid accumulation in adipocytes. These findings suggest a novel role for EZH2 in adipocyte lipid metabolism beyond its reported role as a regulator of adipogenic differentiation.

Results

Reduced EZH2 expression during adipogenic differentiation

To examine the pattern of EZH2 expression during adipogenic differentiation, we conducted a time course experiment using primary human preadipocytes. EZH2 protein was down-regulated early (~70% by day 3) during differentiation of primary human subcutaneous (SQ; Fig. 1, *A* and *B*) and visceral (Fig. S1) preadipocytes. Likewise, mature adipocytes (MA) isolated from murine adipose tissues expressed significantly less EZH2 and RbAP48 (another core component of the PRC2 complex) proteins and a higher level of PPARγ (adipogenic marker) protein, compared with stromal vascular (SV) cells (Fig. 1, *C* and *D*). These findings suggest that adipogenic differentiation is associated with down-regulated expression of EZH2 and other PRC2 core proteins.

EZH2 inhibition induced lipid accumulation but did not repress differentiation of human preadipocytes

EZH2 inhibition was reported to hinder differentiation of murine and human preadipocytes into mature, lipid-laden adipocytes (5, 6). Conversely, treatment with the EZH2 inhibitor, DZNEP, was reported to enhance lipid droplet accumulation in breast cancer cells (15). To dissect the role of EZH2 in regulating adipogenic differentiation and lipid accumulation, human preadipocytes were treated with a highly selective EZH2 pharmacological inhibitor (GSK126, a SAM-competitive EZH2 inhibitor), and adipogenic differentiation was induced. GSK126 is known to inhibit the catalytic site of EZH2 (16), exhibiting over 1000-fold selectivity for EZH2 *versus* 20 other human methyltransferases (17). The efficacy and selectivity of GSK126 were validated by a marked reduction in H3K27me^3 levels (Fig. 2*A*) without significant alterations in H3K4me^3 (Fig. 2*B*) or total protein (Fig. 2*C*) levels, respectively. Interestingly, human preadipocytes treated with GSK126 during *in vitro* differentiation exhibited increased lipid accumulation, as demonstrated by Oil Red O (ORO) staining (Fig. 2*D*) and intracellular triglyceride (Fig. 2*E*) and cholesterol contents (Fig. S6*A*), respectively. Expression of key adipocyte differentiation marker (adiponectin and PPARγ) mRNA (Fig. 2*F*) and protein (Fig. 2, *G* and *H*) was not significantly affected by GSK126 treatment as compared with vehicle-treated cells. These data suggest that inhibition of EZH2 can promote lipid accumulation independent of regulating differentiation in primary human preadipocytes.

Generation of adipocyte-specific EZH2 KO mice

To investigate the role of EZH2 in regulating adipocyte function *in vivo*, we generated adipocyte-specific EZH2 KO mice in which the adiponectin (Adipoq) promoter/regulatory regions drive Cre recombinase, the enzyme responsible for ablating the *Ezh2* gene. Because Adipoq is mainly expressed in mature adipocytes, this model thereby permits tissue-specific EZH2 deletion. The presence of WT/flox EZH2 allele and/or Adipoq-Cre allele in mice was validated via PCR-based genotyping (Fig. S1*A*). Gene expression data from Adipoq-Cre$^+$/EZH2$^{f/f}$ mice confirmed that EZH2 mRNA levels were selectively reduced in mature adipocytes and whole adipose tissues, without significant alterations in adipose-derived SV cells (progenitor-enriched) and most other nonadipose tissues (Fig. S2*B*). As expected, compared with littermate controls (EZH2$^{f/f}$ mice), Adipoq-Cre$^+$/EZH2$^{f/f}$ mice displayed a more dramatic reduction of EZH2 mRNA levels in the mature adipocytes compared with the whole adipose tissues (Fig. S2*B*), suggesting a selective deletion of the EZH2 gene in the mature adipocytes but not in other cell types (*i.e.* fibroblasts, macrophages, progenitor cells, and endothelial cells) within the adipose depots. Interestingly, kidneys isolated from Adipoq-Cre$^+$/EZH2$^{f/f}$ mice displayed a significant reduction in EZH2 mRNA levels (Fig. S2*B*), which may be explained by the expression and secretion of adiponectin by renal tubular epithelial cells, in addition to adipocytes (18). Visceral adipose tissue isolated from Adipoq-Cre$^+$/EZH2$^{f/f}$ mice exhibited a significant reduction in H3K27me^3 modifications compared with that of control mice, confirming reduced EZH2 functional activity (Fig. S2*C*).

Adipocyte-specific EZH2 deletion resulted in adipocyte hypertrophy and reduced plasma VLDL-triglyceride levels, without affecting markers of adipogenic differentiation

Intriguingly, Adipoq-Cre$^+$/EZH2$^{f/f}$ mice consuming standard chow diet displayed increased body weight (Fig. 3*A*) and a strong trend toward greater fat mass (Fig. 3*B*) compared with EZH2$^{f/f}$ controls. Both groups of mice consumed comparable amounts of food, whereas locomotor activity showed a nonsig-

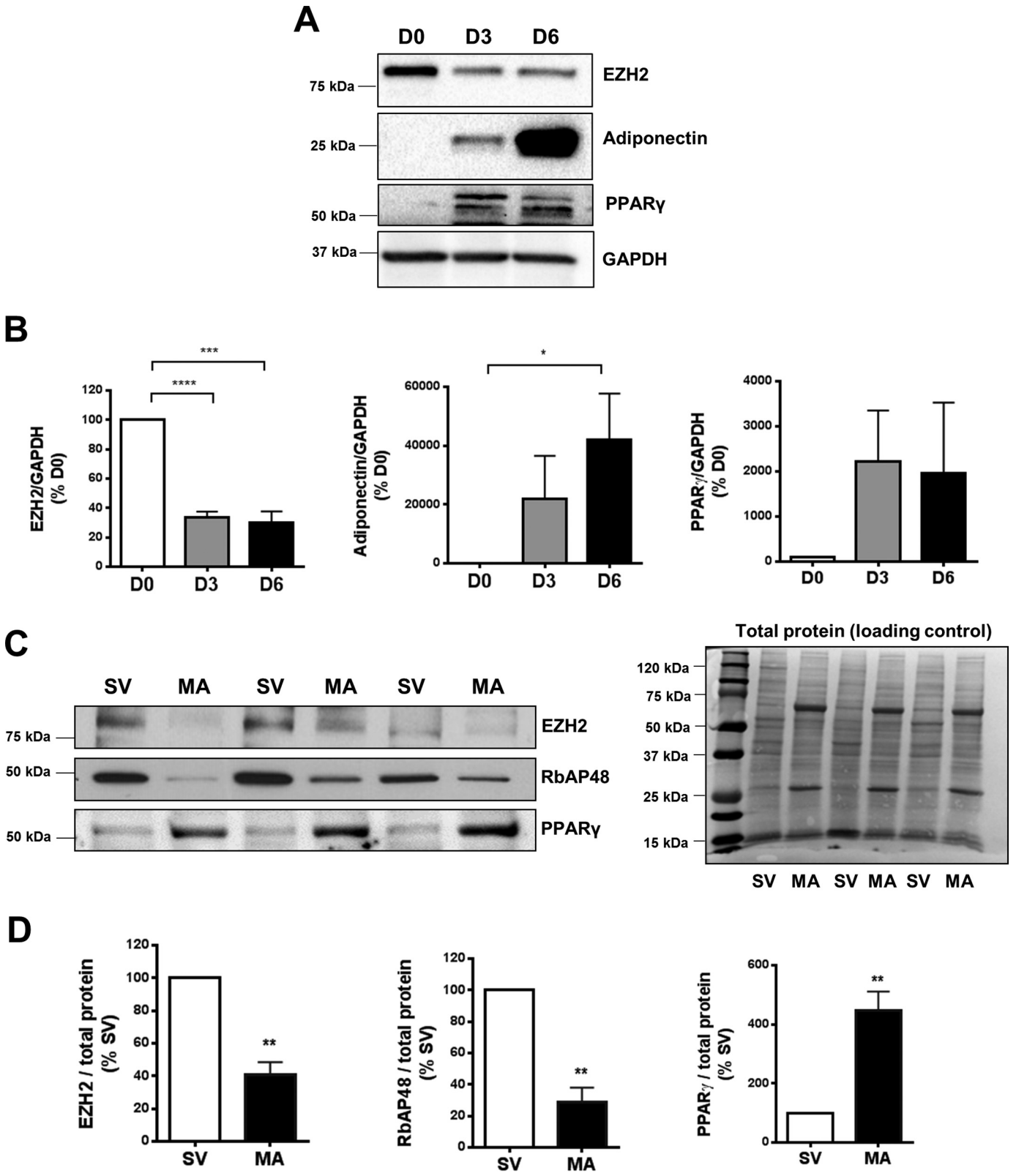

Figure 1. Reduced EZH2 expression during adipogenic differentiation. *A* and *B*, time course of EZH2 protein expression during *in vitro* adipogenic differentiation of human SQ preadipocytes ($n = 4$). Protein expression was determined by Western blotting (*A*) and quantified by densitometry analysis (*B*). Representative Western blotting image (*C*) and densitometry analysis (*D*) of EZH2 and RbAP48 proteins in isolated MA compared with SV fraction from mouse SQ adipose tissues. Individual protein levels were normalized to total protein, respectively ($n = 3$). *, $p < 0.05$; **, $p < 0.01$; ***, $p < 0.001$; ****, $p < 0.0001$. *D0*, undifferentiated; *D3*, 3 days post-adipogenic differentiation; *D6*, 6 days post-adipogenic differentiation. *SV*, stromal vascular; *MA*, mature dipocytes. *Error bars*, S.E.

nificant trend toward a reduction in the Adipoq-Cre^{+}/EZH2$^{f/f}$ mice (Fig. 3*C*). Respiratory exchange ratio, metabolic energy expenditure, CO_2 production, O_2 consumption, heat generation, water consumption, and glucose and insulin tolerance likewise did not differ significantly between the two groups of mice (Fig. S3, *A–H*). Assessment of lipid profiles showed that

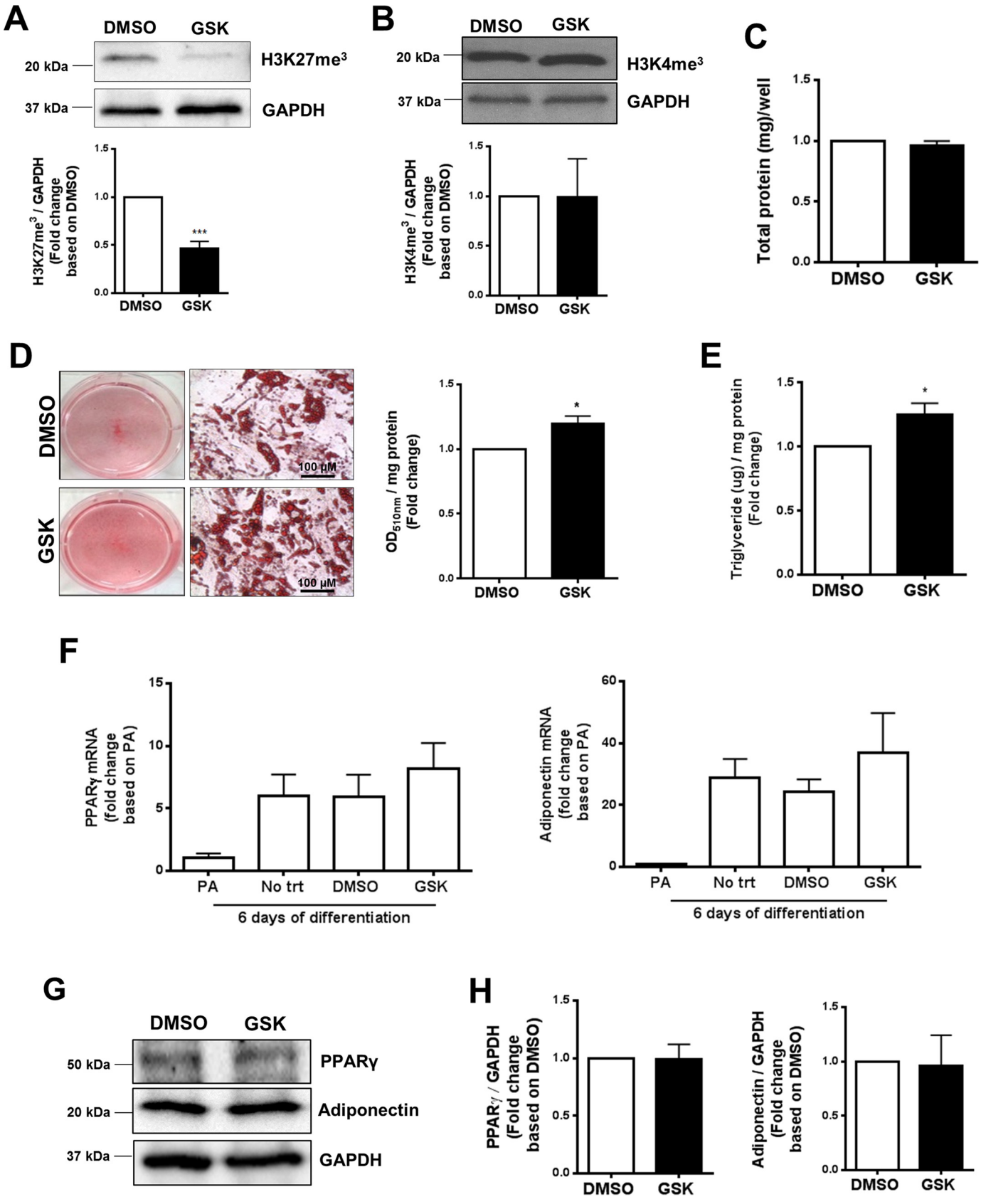

Adipoq-Cre$^+$/EZH2$^{f/f}$ mice displayed lower VLDL-triglyceride (Adipoq-Cre$^+$/EZH2$^{f/f}$ (9 μg) *versus* EZH2$^{f/f}$ (19.5 μg)), with no difference in VLDL-cholesterol, compared with control mice (Fig. 3, *D* and *E*). There was a nonsignificant trend toward reduced total plasma triglyceride (Fig. 3*F*) in Adipoq-Cre$^+$/EZH2$^{f/f}$ *versus* EZH2$^{f/f}$ mice, whereas total plasma cholesterol (Fig. 3*G*) and lipid contents of other plasma lipoprotein species, including intermediate-density lipoprotein (IDL), low-density lipoprotein (LDL) (IDL/LDL-triglyceride: EZH2$^{f/f}$ (18.5 μg) *versus* Adipoq-Cre/EZH2$^{f/f}$ (21 μg)), and high-density lipoprotein (HDL) (Fig. 3, *D* and *E*), were similar in the two groups of mice.

Tissue mass (Fig. 4*A*, indexed to body weight) and fat composition (Fig. S3*I*) of kidney, spleen, liver, heart, lung, and skeletal muscle were unaffected by deletion of EZH2 in adipose tissues. However, SQ fat mass was increased in the Adipoq-Cre$^+$/EZH2$^{f/f}$ mice as compared with EZH2$^{f/f}$ controls (Fig. 4*A*). There were also nonsignificant trends toward increased visceral and brown adipose tissue masses in the Adipoq-Cre$^+$/EZH2$^{f/f}$ mice. Histological analyses (hematoxylin and eosin staining) of SQ adipose tissues demonstrated increased adipocyte cell size in Adipoq-Cre$^+$/EZH2$^{f/f}$ mice compared with control mice (Fig. 4, *B* and *C*). There was also a strong trend toward increased adipocyte cell size in the visceral adipose tissues (Fig. 4*E*). In contrast, there was no significant difference in adipocyte numbers between either SQ (Fig. 4*D*) or visceral adipose depots (Fig. 4*F*) of Adipoq-Cre$^+$/EZH2$^{f/f}$ mice and control mice.

Adipose-specific EZH2 deletion did not affect mRNA expression of key adipocyte differentiation markers (adiponectin and PPARγ) in mature adipocytes isolated from the SQ and visceral adipose tissues (Fig. S4*A*). Moreover, PPARγ and adiponectin protein expression in visceral adipose tissues was not significantly altered by EZH2 deletion in adipocytes (Fig. S4, *B* and *C*). These findings suggest that EZH2 deletion in adipocytes *in vivo* promotes weight gain, adiposity, and adipocyte hypertrophy independent of influencing adipogenic differentiation.

Effects of EZH2 repression on lipolysis, FA uptake, and glucose-stimulated triglyceride accumulation in primary human adipocytes

Adipocyte lipid content is positively regulated by FA uptake/esterification and DNL and negatively regulated by lipolysis. Our *in vitro* and *in vivo* data thus raised the possibility that EZH2 inhibition might directly or indirectly regulate one or more of these metabolic processes to increase lipid content in adipocytes. To investigate whether EZH2 inhibition regulates adipocyte lipolysis, human SQ preadipocytes were treated with either GSK126 (5 μM) or vehicle (DMSO 0.1%), differentiated, and maintained in culture. The mature adipocytes were then treated with or without 3-isobutyl-1-methylxanthine (IBMX) to stimulate lipolysis. We subsequently measured free glycerol release (index of lipolysis) into the culture medium. GSK126 did not significantly influence basal or IBMX-stimulated glycerol release from *in vitro* differentiated human adipocytes (Fig. 5*A*). Intracellular triglyceride content in human adipocytes under basal conditions and following stimulation with IBMX was also unaffected by treatment with GSK126 (Fig. 5*B*). These findings were further verified *in vivo* and *ex vivo* using the Adipoq-Cre$^+$/EZH2$^{f/f}$ mice. Adipoq-Cre$^+$/EZH2$^{f/f}$ mice and control mice injected with 10 mg/kg isoproterenol or saline (control) exhibited no difference in plasma free glycerol levels at 0, 15, and 60 min post-injection (Fig. S5*A*). Moreover, plasma FA levels were comparable between EZH2$^{f/f}$ mice and Adipoq-Cre$^+$/EZH2$^{f/f}$ mice, further suggesting that EZH2 does not affect lipolysis (Fig. S5*B*). For *ex vivo* lipolysis measurement, SQ and visceral fat pads isolated from Adipoq-Cre$^+$/EZH2$^{f/f}$ and control mice were incubated in culture media in the presence or absence of isoproterenol (5 or 10 μM), and free glycerol release (normalized to tissue weights) was subsequently quantified. Similarly, adipose tissue free glycerol release, under basal and stimulated lipolytic conditions, was unaffected by adipocyte-specific EZH2 gene deletion (Fig. S5, *D* and *E*). Interestingly, phosphorylation of hormone-sensitive lipase, an enzyme that regulates lipolysis, was increased in adipose tissues of Adipoq-Cre$^+$/EZH2$^{f/f}$ mice as compared with EZH2$^{f/f}$ mice (Fig. S5*C*), functional consequences of which remain to be determined.

Next, we investigated the role of EZH2 in regulating FA uptake. Exogenous FA (oleic acid) conjugated with BSA was added to human adipocytes treated with either GSK126 (5 μM) or vehicle control (DMSO 0.1%) 14–21 days post-adipogenic differentiation. Then extracellular oleic acid concentration in the culture medium was determined over 6 h at different time points. Across all time points, GSK126 treatment did not influence the disappearance of oleic acid from the medium (Fig. 5*C*), suggesting that FA uptake *per se* was not affected by EZH2 inhibition. In separate experiments conducted on cells at an earlier state of adipogenic differentiation, we quantified triglyceride levels following incubation with oleic acid. The increase in intracellular triglycerides over baseline (albumin control) in cells incubated with oleic acid was not affected by treatment with GSK126 (Fig. S5, *F* and *G*), suggesting that inhibition of EZH2 did not increase adipocyte lipids by augmenting uptake or esterification of exogenous FA.

To investigate the role of EZH2 in regulating glucose-stimulated triglyceride accumulation, human preadipocytes treated with either GSK126 or vehicle were differentiated in high-glucose and serum-free (FA-deficient) medium. Under these conditions, GSK126-treated adipocytes displayed slightly reduced ORO staining compared with vehicle-treated adipocytes (Fig. 5*D*), whereas intracellular triglyceride content was similar in the two groups of cells (Fig. 5*E*). Moreover, mRNA expression

Figure 2. Effect of EZH2 inhibitor on lipid accumulation and adipogenic markers expression in human adipocytes. *In vitro* differentiated (6–12 days) primary human SQ preadipocytes were treated with EZH2 inhibitor (GSK126, 5 μM) or vehicle (DMSO). *A* and *B*, validation of GSK126 efficacy and selectivity via measurements of H3K27me^3 (*A*) and H3K4me^3 (*B*) protein levels. *C*, total intracellular protein concentration per well. *D*, representative appearance of cytoplasmic lipid droplets (ORO staining) 6 days post-adipogenic differentiation. Neutral lipid accumulation was quantified by spectrophotometry ($n = 4$). *E*, intracellular triglyceride content ($n = 6$). Shown are adipogenic marker (PPAR-γ and adiponectin) mRNA (*F*) and protein (*G* and *H*) levels 6 days post-adipogenic differentiation. *, $p < 0.05$; ***, $p < 0.001$; *PA*, preadipocytes. *Error bars*, S.E.

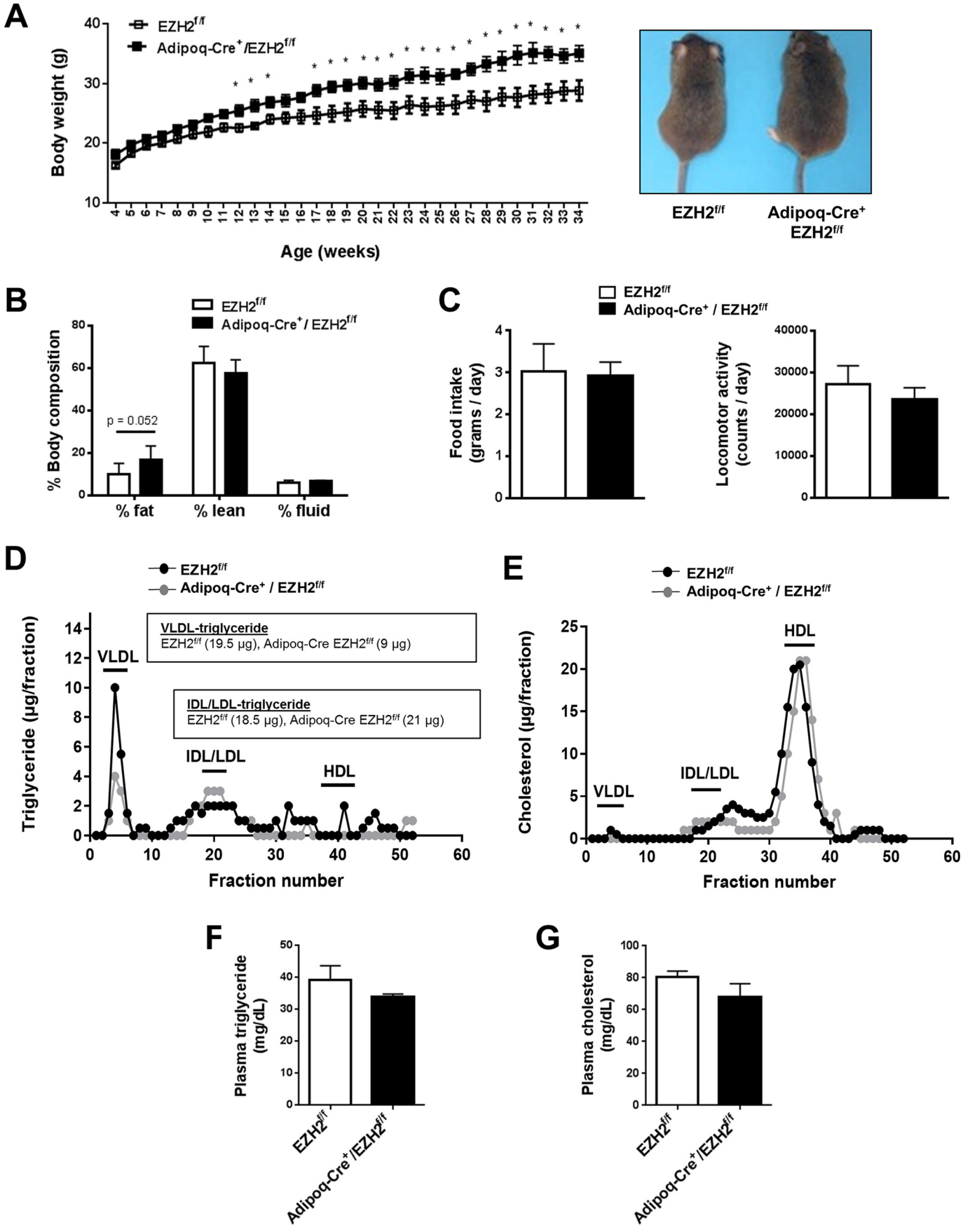
A
EZH2f/f
Adipoq-Cre+/EZH2f/f
Body weight (g)
Age (weeks)
EZH2f/f
Adipoq-Cre+ EZH2f/f
B
EZH2f/f
Adipoq-Cre+ / EZH2f/f
% Body composition
p = 0.052
% fat
% lean
% fluid
C
EZH2f/f
Adipoq-Cre+ / EZH2f/f
Food intake (grams / day)
Locomotor activity (counts / day)
D
EZH2f/f
Adipoq-Cre+ / EZH2f/f
Triglyceride (µg/fraction)
VLDL-triglyceride
EZH2f/f (19.5 µg), Adipoq-Cre EZH2f/f (9 µg)
IDL/LDL-triglyceride
EZH2f/f (18.5 µg), Adipoq-Cre EZH2f/f (21 µg)
VLDL
IDL/LDL
HDL
Fraction number
E
EZH2f/f
Adipoq-Cre+ / EZH2f/f
Cholesterol (µg/fraction)
VLDL
IDL/LDL
HDL
Fraction number
F
Plasma triglyceride (mg/dL)
EZH2f/f
Adipoq-Cre+/EZH2f/f
G
Plasma cholesterol (mg/dL)
EZH2f/f
Adipoq-Cre+/EZH2f/f

of key DNL gene markers (fatty acid synthase (*FASN*), acetyl-CoA carboxylase α (*ACCa*), sterol regulatory element–binding protein 1 (*SREBP1*), carbohydrate-responsive element-binding protein (*CHREBP1*) (also known as MLX-interacting protein-like (MLXIPL), and stearoyl-CoA desaturase 1 (*SCD1*)) was unaffected by treatment with GSK126 (Fig. 5*F*). Although DNL was not directly quantified, these data nevertheless suggest that GSK126 does not promote adipocyte lipid accumulation by increasing glucose-stimulated triglyceride accumulation.

Effects of EZH2 repression on lipoprotein-dependent lipid uptake

Our *in vivo* data demonstrated that adipocyte-specific EZH2 deletion resulted in reduced plasma VLDL-triglyceride levels (Fig. 3, *D* and *E*). Notably, adipocytes can take up lipid from lipoproteins, in particular VLDL, thereby increasing their intracellular lipid content. To test whether EZH2 inhibition could potentially increase adipocyte lipid content by enhancing lipoprotein-dependent lipid uptake, we first performed experiments using lipoprotein-depleted serum. Under these conditions, GSK126 failed to significantly increase adipocyte triglyceride levels, suggesting an obligatory role for lipoproteins in conferring the effects of EZH2 inhibition on lipid accumulation in adipocytes (Fig. 6*A*). We next examined the role of EZH2 in regulating lipoprotein-dependent lipid uptake in primary human adipocytes. VLDL labeled with 1,1′-dioctadecyl-3,3,3′,3′-tetramethylindocarbocyanine perchlorate (Dil) was added to human adipocytes treated with either GSK126 (5 μM) or vehicle control, and intracellular fluorescence was quantified. Interestingly, Dil-VLDL uptake by human adipocytes was increased by EZH2 inhibition (Fig. 6*B*). To determine whether EZH2 gene deletion would likewise augment lipoprotein-dependent lipid uptake in murine adipocytes, we isolated preadipocytes from the Adipoq-Cre$^+$/EZH2$^{f/f}$ mice and control mice. Following *in vitro* differentiation, we incubated the cells with Dil-VLDL and quantified fluorescence. As was observed in human adipocytes treated with the EZH2 inhibitor, genetic deletion of EZH2 significantly increased Dil-VLDL uptake by murine adipocytes (Fig. 6*C*).

Adipocyte-expressed *ApoE* has been reported to play an important role in VLDL uptake *in vitro* (2). In addition, *ApoE* was previously predicted as a gene target of EZH2 (19). Accordingly, human adipocytes treated with GSK126 exhibited increased *ApoE* gene expression as compared with vehicle control (Fig. 6*D*). Likewise, *ApoE* gene expression in adipocytes isolated from Adipoq-Cre$^+$/EZH2$^{f/f}$ mice was increased as compared with those from control mice (Fig. 6*E*). Furthermore, Dil-VLDL uptake induced by EZH2 inhibition was abolished in *ApoE*-deficient adipocytes (Fig. 6*F*).

EZH2 inhibition could potentially induce lipid accumulation via internalization of VLDL particles and/or uptake of free lipid hydrolyzed extracellularly by lipoprotein lipase (LPL). Thus, we quantified cellular levels of cholesterol and ApoB-100 protein, a major protein constituent of VLDL, following incubation with VLDL. GSK126 treatment increased both cholesterol and ApoB-100 levels in human adipocytes (Fig. S6, *A* and *B*). Conversely, neither LPL protein expression nor activity was affected by treatment with GSK126 (Fig. S6*C*). These findings support the notion that inhibition of EZH2 promotes VLDL particle internalization in adipocytes. Taken together, these data suggest that EZH2 repression promotes extracellular lipoprotein-dependent lipid accumulation in adipocytes, at least in part by up-regulating adipocyte *ApoE* expression and lipoprotein internalization.

Discussion

EZH2 has been suggested to play an obligatory role in promoting adipogenic differentiation. On the other hand, inhibition of EZH2 (which has been identified as a key molecule for oncogenesis and a target of cancer therapy) was reported to induce lipid accumulation in other types of cells. Here, we undertook a systematic approach to dissect the role of EZH2 in regulating adipogenic differentiation and lipid metabolism. Major findings of this study are that 1) EZH2 is down-regulated during adipogenic differentiation; 2) EZH2 inhibition induced lipid accumulation in adipocytes independent of affecting adipogenic differentiation; 3) adipocyte-specific EZH2 deletion in mice resulted in increased body weight and adiposity and reduced plasma VLDL-triglyceride levels; 4) EZH2 inhibition did not induce adipocyte lipid accumulation by influencing lipolysis, glucose-stimulated triglyceride accumulation, or FA acid uptake; and 5) EZH2 inhibition induced extracellular lipoprotein-dependent lipid uptake via up-regulating *ApoE* gene expression in adipocytes, thus establishing a novel mechanism whereby EZH2 regulates lipid metabolism.

Epigenetic mechanisms, including histone modifications, are postulated to regulate expression of genes pivotal to the adipogenic differentiation program. Previously, EZH2 was proposed to function as a positive regulator of adipogenic differentiation in murine adipose progenitor cells (5); however, studies involving human cells to date are very limited. In this study, we observed a dramatic down-regulation of EZH2 during adipogenic differentiation, which may not be universal for all adipocyte progenitor cell lineages and/or species. For instance, EZH2 expression reportedly remained constant in human bone marrow–derived mesenchymal stem cells (MSCs), but increased in mouse MSCs, during adipogenic differentiation (8, 9), suggesting that distinct epigenetic signatures drive cell type–specific gene expression and contribute to their unique cellular identities in a species-dependent manner. Interestingly, our results with human primary adipocytes demonstrated that pharmacological inhibition of EZH2 using a specific inhibitor, GSK126, did not impede adipogenic differentiation, but rather

Figure 3. Characterization of adipose-specific EZH2 KO mice. Adipoq-Cre$^+$/EZH2$^{f/f}$ and EZH2$^{f/f}$ littermate control mice were fed a standard chow diet for 34 weeks (n = 4–6). *A*, body weights and representative gross morphology of 34-week-old mice. *B*, whole-body fat and lean composition by noninvasive NMR. *C*, average food intake and locomotor activity over 72 h monitored via CLAMS. *D* and *E*, representative plasma lipoprotein profile measured via FPLC using pooled plasma (0.22 ml) from three Adipoq-Cre$^+$/EZH2$^{f/f}$ mice and six EZH2$^{f/f}$ mice. Total plasma (*F*) triglyceride and cholesterol levels (*G*). *, $p < 0.05$. *Adipoq*, adiponectin; *VLDL*, very low-density lipoprotein; *IDL*, intermediate-density lipoprotein; *LDL*, low-density lipoprotein; *HDL*, high-density lipoprotein. *Error bars*, S.E.

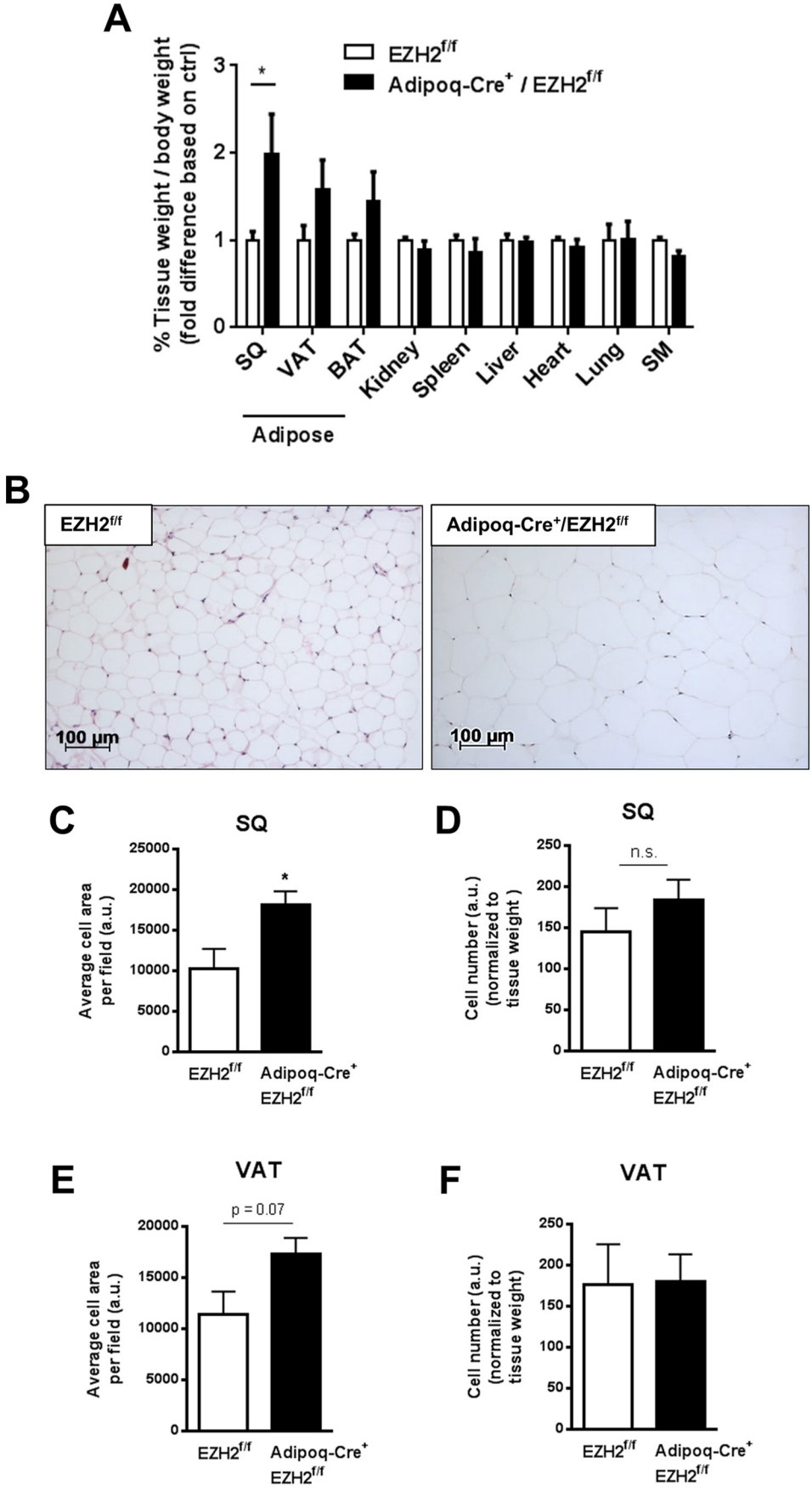
A
% Tissue weight / body weight (fold difference based on ctrl)
EZH2f/f
Adipoq-Cre+ / EZH2f/f
*
SQ
VAT
BAT
Kidney
Spleen
Liver
Heart
Lung
SM
Adipose
B
EZH2f/f
Adipoq-Cre+/EZH2f/f
100 μm
100 μm
C
SQ
Average cell area per field (a.u.)
*
EZH2f/f
Adipoq-Cre+ EZH2f/f
D
SQ
Cell number (a.u.) (normalized to tissue weight)
n.s.
EZH2f/f
Adipoq-Cre+ EZH2f/f
E
VAT
Average cell area per field (a.u.)
p = 0.07
EZH2f/f
Adipoq-Cre+ EZH2f/f
F
VAT
Cell number (a.u.) (normalized to tissue weight)
EZH2f/f
Adipoq-Cre+ EZH2f/f

induced lipid accumulation. These findings differ from those reported in another study in human subcutaneous preadipocytes, wherein GSK126 (2 μM) was reported to impair adipogenic differentiation and lipid droplet formation (20). The reasons for these discrepant findings are unclear. Whereas the data reported in the present study were obtained using a higher concentration of GSK126 (5 μM), dose-response studies failed to demonstrate divergent results at lower concentrations (not shown). We also considered whether differences in timing of application of the inhibitor might have been contributory; however, varying the timing of exposure to GSK126 to mimic the protocol reported (20) did not result in impaired adipogenic differentiation (not shown). It is conceivable that differences in the individual sites of acquisition of adipose tissues could explain the discrepant findings. However, we examined subcutaneous adipose tissues obtained from both abdominal and thoracic regions of humans and observed similar results (not shown). Whereas the methods of isolation of adipose progenitors were similar in the two studies, subtle differences in cell populations and/or culture conditions may be contributory. For example, in the present study, progenitor cells were not freeze-thawed and were used at early passage numbers for all studies.

It is noteworthy that our findings in human adipogenic differentiation *in vitro* mirrored the results obtained with the adipocyte-specific EZH2 KO mice. Indeed, the adipocyte-specific EZH2 KO mice exhibited no differences in adipogenic gene expression as compared with littermate control mice, although it is important to point out that these mice were studied at a young age and under standard chow-diet feeding; it is possible that the impact of EZH2 gene deletion on adipogenic differentiation *in vivo* differs depending on age and/or diet, which merits further investigation. Regardless, under these conditions, the subcutaneous adipocytes of EZH2 KO mice were larger in size, without significant changes in adipocyte number, leading to greater subcutaneous fat mass that was not explained by differences in feeding behavior, activity, or metabolic energy expenditure. Reduced VLDL-triglyceride levels in the adipocyte-specific EZH2 KO mice suggest that lipid partitioning from the plasma to the adipocyte pool may explain these subtle differences in body composition, consistent with the *in vitro* findings in human and mouse cells. Whereas a variety of lipoprotein species, including chylomicrons and IDL, also carry triglycerides, this study was particularly focused on VLDL uptake because VLDL carries 90% of the serum triglycerides in the fasting state (21). Moreover, FPLC measurements using plasma from fasting animals demonstrated a reduction in VLDL-triglyceride upon adipocyte-specific EZH2 gene deletion, without demonstrable effects on other lipoprotein species. The potential effects of EZH2 inhibition on lipoprotein particle number and size remain to be determined. Nevertheless, the findings of this study suggest a novel role for EZH2 in governing adipocyte lipid storage and metabolism via biological mechanisms distinct from adipogenic differentiation *per se*.

Adipocyte lipid content is dynamically regulated, reflecting the balance between energy storage and expenditure. Lipid catabolism, the breakdown of triacylglycerols into free glycerol and FAs, is a fundamental process in energy expenditure. Under normal conditions, the basal lipolytic rate in adipocytes is relatively low, consistent with its essential function as an energy storage tissue. On the other hand, excess nonlipid substrates (*i.e.* carbohydrate and protein) are converted into lipids, a more efficient form of storage, through DNL. Moreover, the ability of white adipocytes to efficiently take up dietary long-chain FA is essential to their physiological function in energy storage. In healthy human subjects, dietary FA is the major source contributing to adipocyte intracellular lipid stores (*i.e.* triglycerides, cholesterol esters, and phospholipids). Our data, however, indicate that EZH2 inhibition does not affect adipocyte lipolysis, glucose-stimulated triglyceride accumulation, or FA uptake. Triglyceride-rich lipoprotein internalization into adipocytes also modulates cellular lipid balance (22), and this process is facilitated by *ApoE* (23, 24). Whereas *ApoE* is produced by various organs and cell types, circulating *ApoE* is mainly derived from the liver. *ApoE* is nevertheless highly expressed in adipocytes and contributes to adipocyte triglyceride turnover and VLDL metabolism (2, 3). Notably, mice globally deficient in *ApoE* gained less body weight, concomitant with lower fat mass and smaller adipocytes, as compared with WT mice (4, 23, 24). Adipocyte-specific deletion of *ApoE* in mice likewise resulted in less adiposity and smaller adipocytes, without affecting circulating *ApoE* levels (3), suggesting that adipocyte-derived *ApoE* plays an important role in adipose tissue lipid metabolism. Here, we identify a role for EZH2 in regulating *ApoE*-mediated lipoprotein uptake in adipocytes. This conclusion is supported by the following observations: 1) EZH2 inhibition significantly augmented lipid accumulation in human adipocytes only when cultured in lipoprotein-replete medium; 2) both lipoprotein-dependent lipid uptake and *ApoE* gene expression in human and mouse adipocytes were significantly augmented by EZH2 inhibition; and 3) EZH2 inhibition failed to augment lipid accumulation in *ApoE*-deficient murine adipocytes. Previously, RNA-Seq studies in retina-specific EZH2 KO mice identified *ApoE* as one of the top 15 genes up-regulated by EZH2 deficiency (19), suggesting that *ApoE* is a potential target of EZH2 not only in adipocytes, but also in other cell types and tissues. Notably, *ApoE* is also expressed in numerous cancer cells and was reported to promote proliferation and survival of ovarian and lung tumor cells (25, 26). Such up-regulated expression of *ApoE* by EZH2 inhibition could potentially mitigate the anti-tumor effects of EZH2 inhibitors currently under investigation in cancer clinical trials, which merits further consideration.

Figure 4. Effects of adipose-specific deletion of EZH2 on adipocyte cell size/number and adipogenic markers. *A*, weights of various tissues isolated from Adipoq-Cre$^+$/EZH2$^{f/f}$ and EZH2$^{f/f}$ mice, respectively. *B*, representative histological image of adipocyte size of SQ adipose tissues. Adipocyte size and number were quantified in SQ (*C* and *D*) and visceral adipose tissues (*E* and *F*), respectively. *, $p < 0.05$; *n.s.*, not significant; *VAT*, visceral adipose tissue; *BAT*, brown adipose tissue; *SM*, skeletal muscle. *Error bars*, S.E.

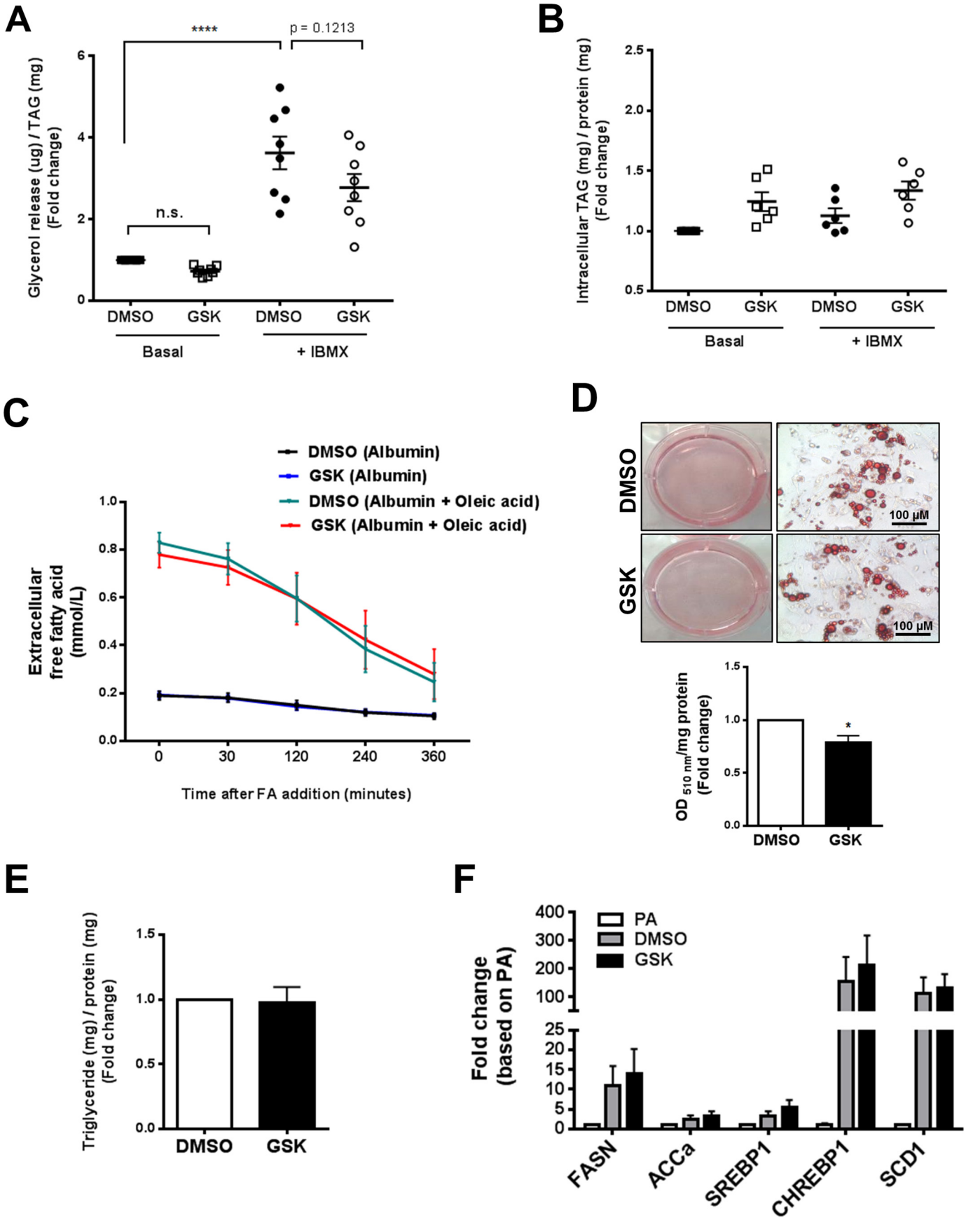
A
****
p = 0.1213
n.s.
Glycerol release (ug) / TAG (mg)
(Fold change)
DMSO
GSK
DMSO
GSK
Basal
+ IBMX
B
Intracellular TAG (mg) / protein (mg)
(Fold change)
DMSO
GSK
DMSO
GSK
Basal
+ IBMX
C
DMSO (Albumin)
GSK (Albumin)
DMSO (Albumin + Oleic acid)
GSK (Albumin + Oleic acid)
Extracellular
free fatty acid
(mmol/L)
Time after FA addition (minutes)
D
DMSO
GSK
100 μM
100 μM
OD 510 nm/mg protein
(Fold change)
DMSO
GSK
E
Triglyceride (mg) / protein (mg)
(Fold change)
DMSO
GSK
F
PA
DMSO
GSK
Fold change
(based on PA)
FASN
ACCa
SREBP1
CHREBP1
SCD1

EZH2 functions as a multifaceted protein involved in various biological processes including development and survival; however, its function in glucose and lipid metabolism has only been recently examined. Pang *et al.* (27) reported that EZH2 promotes tumorigenesis and malignant progression of glioblastoma cells in part by activating aerobic glycolysis (Warburg effect) through an EAF2-HIF1α axis. EZH2 overexpression in glioblastoma cells also induced glucose uptake, glycolytic enzyme expression and activity, and lactate production. These findings are consistent with other studies showing that EZH2 expression correlated with glycometabolism-related genes and that EZH2 positively regulated aerobic glycolysis in human prostate cancer cell lines and glioma cells (28, 29). Whereas studies elucidating the role of EZH2 in regulating lipid metabolism are limited, observational studies have indicated that breast cancer cells and hepatocytes accumulate cytoplasmic lipid droplets in response to EZH2 inhibitor (DZNEP) treatment (14, 15). These interesting findings are congruent with our observations in mammalian adipocytes wherein disruption in EZH2 function resulted in increased intracellular lipids in human adipocytes *in vitro* and increased lipid volume in mouse adipose tissues *in vivo*. Whereas we report a novel role for EZH2 in *ApoE*-mediated lipoprotein-dependent lipid metabolism, potential functions of EZH2 in other important metabolic pathways, such as glycolysis, β-oxidation, lipid droplet budding from the endoplasmic reticulum, and lipotoxicity in mammalian adipocytes, remain to be investigated.

In conclusion, our findings provide new insight into the potential mechanisms whereby EZH2 regulates lipid metabolism, beyond its reported role as a regulator of adipogenic differentiation. Our findings characterizing EZH2 function in adipocytes derived from human subjects, and in the novel adipocyte-specific EZH2 KO mouse model, may be relevant to the fields of lipidology and cancer biology. Moreover, these findings could have clinical implications for humans, as EZH2 inhibitors are currently being tested in clinical trials in patients with various malignancies.

Experimental procedures

Animals

EZH2 floxed ($EZH2^{f/f}$) mice (Jackson Laboratories) contain two loxP sites flanking exons 14–15 of the EZH2 gene (30). Exons 14 and 15 encode part of the catalytic SET domain of the EZH2 gene; their deletion introduces a frameshift and subsequent termination mutation, which effectively obliterates EZH2 catalytic domain. EZH2 gene was conditionally ablated in adipocytes by mating $EZH2^{f/f}$ mice with Adipoq-Cre mice (Jackson Laboratories). These crosses generated littermate controls (Adipoq-Cre^{-}/$EZH2^{f/f}$ or Adipoq-Cre^{-}/$EZH2^{f/+}$) or adipose-specific KO (Adipoq-Cre^{+}/$EZH2^{f/f}$) mice. Seven-week-old male Adipoq-Cre^{+}/$EZH2^{f/f}$ mice and $EZH2^{f/f}$ control mice were fed a standard chow diet (Harlan Teklad, LM-485) for 27 weeks. Both diet and water were provided *ad libitum*. The institutional animal care and use committee of the Medical College of Georgia at Augusta University approved all animal experiments.

Preparation of human adipose tissues

Human adipose tissues were collected from patients undergoing cardiothoracic and bariatric surgeries. The study protocol was approved by the institutional review boards of the Medical College of Georgia at Augusta University. This study was carried out in accordance with the recommendations of the Declaration of Helsinki.

Isolation of adipocytes and preadipocytes and in vitro adipogenic differentiation

SV cells (preadipocyte-enriched) and *in vivo* mature adipocytes were isolated from SQ or visceral adipose tissues from humans or mice as previously described (31). Briefly, adipose tissues were thoroughly minced, digested with collagenase type I (Worthington), filtered, and centrifuged to separate floating mature adipocytes from the pelleted SV cells. Mature adipocytes were immediately flash-frozen in liquid nitrogen and stored at −80 °C for further analyses. SV pellets were resuspended, plated, and grown in preadipocyte growth medium (Cell Applications). The cells were expanded up to four passages in culture and differentiated in the presence of adipocyte differentiation medium (Cell Applications) with or without EZH2 inhibitor GSK126 (5 μM). Media and pharmacological treatments were replaced every 3 days.

Quantitative PCR

Total RNA from cells or tissues was extracted using the RNeasy Lipid Tissue Mini Kit (Qiagen). Real-time quantification of mRNA levels was performed using the Brilliant II SYBR Green QPCR kit (Agilent Technologies) per the manufacturer's instructions. Normalized *Ct* values were subjected to statistical analysis, and -fold difference was calculated by the $\Delta\Delta Ct$ method as described previously.

Western blotting

Total cellular proteins were extracted using radioimmune precipitation assay buffer (Thermo Scientific) containing protease inhibitor mixture (Sigma). Proteins (30–50 μg) were separated on an SDS-polyacrylamide gel, transferred to nitrocellulose membranes, and probed with appropriate antibodies, and blots were subsequently developed using the

Figure 5. Effects of EZH2 repression on *in vitro* lipolysis, FA uptake, and glucose-stimulated triglyceride accumulation in primary human adipocytes. *A* and *B*, lipolytic characterization of human adipocytes treated with either GSK126 or vehicle control. Free glycerol release (*A*, index of lipolysis, $n = 8$) and intracellular triglyceride (*B*) under basal and 200 μM IBMX-stimulated states ($n = 6$). Data were normalized to cell triglyceride levels in unstimulated cells. *C*, time course of extracellular FA (oleic acid) uptake in human adipocytes treated with either GSK126 or vehicle. *D*, representative appearance of cytoplasmic lipid droplets (ORO staining) in human adipocytes treated with either GSK126 or vehicle control and maintained in high-glucose (5 mM)/serum-free medium ($n = 4$). Neutral lipid accumulation was quantified by spectrophotometry (510 nm). *E*, intracellular triglyceride content. *F*, mRNA expression of key DNL markers was determined by qPCR. ****, $p < 0.0001$; *n.s.*, not significant; *TAG*, triglyceride; *FASN*, fatty acid synthase; *ACCa*, acetyl-CoA carboxylase α; *SREBP1*, sterol regulatory element–binding protein 1; *CHREBP1*, carbohydrate-responsive element-binding protein (also known as MLX-interacting protein-like (MLXIPL)); *SCD1*, stearoyl-CoA desaturase 1. *Error bars*, S.E.

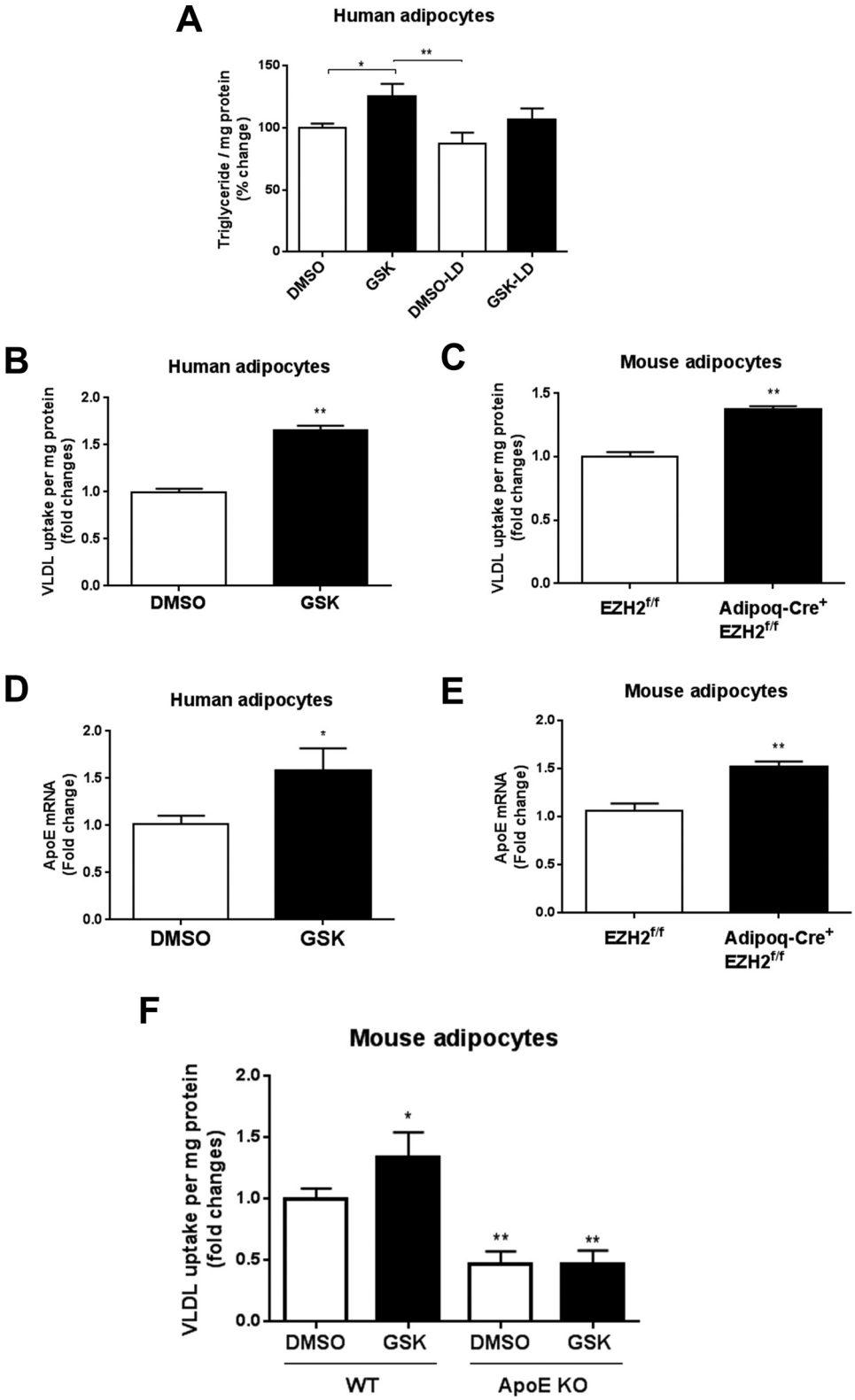

Figure 6. Effects of EZH2 inhibition on lipoprotein uptake and *ApoE* expression in adipocytes. *A*, intracellular triglyceride levels in adipocytes cultured with lipoprotein-deficient medium. Fluorescent Dil-VLDL internalization was measured in human (*B*) and mouse adipocytes (*C*) treated with GSK126 or vehicle. Shown is *ApoE* mRNA expression in human (*D*) and mouse adipocytes (*E*) treated with GSK126 or vehicle. *F*, fluorescent Dil-VLDL internalization in WT and *ApoE*-deficient adipocytes treated with GSK126 or vehicle. *, $p < 0.05$; **, $p < 0.01$; *LD*, lipoprotein-deficient. *Error bars*, S.E.

ECL system (Thermo Scientific). The following primary antibodies were used: EZH2, SUZ12 (Cell Signaling), adiponectin, RbAP48 (Abcam), PPARγ (Santa Cruz Biotechnology, Inc.), trimethyl-histone H3 (Lys-27), and trimethyl-histone H3 (Lys-4) (Millipore), glyceraldehyde-3-phosphate dehydrogenase (Ambion).

Oil Red O staining and intracellular triglyceride measurements

Neutral lipids, stained with ORO, were measured as described previously (32). Briefly, cells were washed with PBS and fixed with 4% paraformaldehyde for 1 h. Then cells were washed with ddH_2O and incubated with ORO working solution (3 parts 0.4% ORO stock solution to 2 parts ddH_2O) for 10 min. After incubation, cells were washed with ddH_2O and imaged under light microscopy, and optical density (510 nm) was measured by a spectrophotometer. Intracellular triglyceride concentration *in vitro* was determined by first lysing cells in radioimmune precipitation assay lysis buffer followed by using a triglyceride measurement kit per the manufacturer's instructions (Thermo Scientific). Triglyceride values were normalized to protein amount.

Body fat composition, food intake, and locomotor activity measurements in mice

Body weights were obtained weekly in mice throughout the duration of the studies as described previously (33). Body fat composition was measured in 34-week-old conscious male mice using NMR spectroscopy (Bruker Minispec LF90II) per the manufacturer's instructions. Food intake and locomotor activity were determined using a comprehensive laboratory animal monitoring system (CLAMS, Columbus Instruments, Columbus, OH) for 4 days (24 h of acclimation, followed by 72 h of measurement) per the manufacturer's instructions.

Plasma lipids and FPLC

Plasma cholesterol and triglycerides were measured using Infinity cholesterol and triglyceride kits (Thermo Fisher Scientific). Plasma lipoprotein profile were determined as described previously (34). Briefly, pooled plasma from three Adipoq-Cre^+ $EZH2^{f/f}$ mice and six $EZH2^{f/f}$ control mice were subjected to FPLC gel filtration on two Superose 6 columns connected in series.

Histology and quantification of adipocyte cell number and size

Murine adipose tissues (inguinal subcutaneous and epididymal) were fixed by immersion in neutral buffered formalin (10%), dehydrated in ethanol, transferred to xylene solution, and embedded in paraffin. Histological sections were stained with hematoxylin and eosin. Adipocyte cell area and number were evaluated by computer-assisted morphometric analysis using Adiposoft (35). Adipocyte cell number was normalized to tissue weight.

Glucose tolerance test

Glucose levels were repeatedly measured from tail veins at 0, 10, 20, 30, 40, 50, 60, 70, 80, 90, 100, and 120 min after intraperitoneal injection of glucose at 2 g/kg body weight in 12-h-fasted mice using glucose strips as described previously (36).

Insulin tolerance test

Insulin sensitivity was assessed by measurement of plasma glucose from tail veins at 0, 10, 20, 30, 40, 50, 60, 70, 80, and 90 min after intraperitoneal injection of 0.75 units/kg body weight of human insulin (Novo Nordisk) in 6-h-fasted mice as described previously (36).

In vitro lipolysis measurement

In vitro differentiated primary human adipocytes were starved overnight (15–18 h) in adipocyte starvation medium (Cell Applications). The next day, the medium was switched to DMEM containing 2% fatty acid–free BSA; basal or stimulated lipolysis was assessed using vehicle control (0.1% DMSO) or 200 μM IBMX, respectively. After 4 h of treatment, glycerol released into the culture medium was quantified and normalized to total intracellular triglyceride levels.

Glucose-stimulated triglyceride measurement assay

Primary human SQ preadipocytes were treated with GSK126 (5 μM) or vehicle (DMSO 0.1%) and then differentiated into mature adipocytes using serum-free medium (DMEM/F12, 4.5 g/liter glucose, 5 μg/ml human insulin, 0.5 μM dexamethasone, 250 μM IBMX, 100 μM indomethacin) for 9 days and maintained in culture for another 6 days in maintenance medium (DMEM/F12 medium, 10 μg/μl insulin). Media and pharmacological treatments were replaced every 3 days. Then adipocytes were fixed for ORO staining or processed for measurements of mRNA, protein, or intracellular triglyceride levels.

Fatty acid uptake assay

Primary human SQ preadipocytes, treated with either GSK126 (5 μM) or vehicle (0.1% DMSO), were studied during early and late stages of adipocyte maturation. Human preadipocytes were differentiated and maintained in culture for a total of 4 days (early stage) or 14–21 days (late stage) post-differentiation. Then mature adipocytes were treated with either FA-free BSA-conjugated oleic acid (1000 μM) (1:10 BSA/oleic acid molar ratio) or control (10% FA-free BSA only) in DMEM. Subsequently, 30 μl of culture medium was collected at 0, 30, 60, 120, 240, and 360 min post-BSA-conjugated oleic acid treatment. Nonesterified fatty acid concentration in the media was determined using an assay kit (WAKO) per the manufacturer's instructions and normalized to protein amount.

Lipoprotein-free serum assay

Primary human SQ preadipocytes, treated with either GSK126 (5 μM) or vehicle (DMSO 0.1%), were cultured in adipocyte differentiation/maintenance media containing 10% lipoprotein-deficient serum or matched-control serum for 6 days. Intracellular triglyceride was measured using a triglyceride kit per the manufacturer's instructions (Thermo Scientific). Intracellular triglycerides were normalized to protein amount.

Dil-VLDL uptake assay

Primary human SQ preadipocytes were treated with either GSK126 (5 μM) or vehicle (0.1% DMSO) and then differentiated into mature adipocytes for a total of 6–10 days. Then maintenance media were replaced with media containing 10% lipoprotein-deficient serum. Purified human VLDL labeled fluorescently with Dil (Kalen Biomedical, LLC) were subsequently added extracellularly at a concentration of 200 μg/ml per well. Six h post-Dil-VLDL incubation, intracellular fluorescence

intensity was determined via fluorescence spectrophotometry (excitation, 530/25 nm; emission, 590/35 nm). Fluorescence intensity was normalized to protein amount. Unlabeled human VLDL was used for measurement of adipocyte cholesterol levels (cholesterol E test kit, Fujifilm Wako Pure Chemical Corp.) and ApoB-100 protein levels under the same conditions.

Statistical analysis

Data are expressed as mean ± S.E. Student's *t* test and two-way analysis of variance were used for comparisons between groups. GraphPad Prism version 7 software was used for these statistical calculations. *, $p < 0.05$ was considered significant; **, $p < 0.01$; ***, $p < 0.001$; ****, $p < 0.0001$.

Author contributions—N. K. Y., D. Y. H., and N. L. W. conceptualization; N. K. Y., C. G., A. Z., B. G., D. K., T. W. B., M. O., D. Y. H., and H. W. K. data curation; N. K. Y. software; N. K. Y., C. G., A. Z., B. G., D. K., T. W. B., M. O., D. Y. H., H. W. K., and N. L. W. formal analysis; N. K. Y., H. W. K., and N. L. W. supervision; N. K. Y., Y. L. T., H. W. K., and N. L. W. validation; N. K. Y., C. G., A. Z., S. A., B. G., Y. L. T., W. C., D. Y. H., H. W. K., and N. L. W. investigation; N. K. Y. and H. W. K. visualization; N. K. Y., A. Z., Y. L. T., W. C., D. S., V. P., R. H., X.-Y. L., D. Y. H., H. W. K., and N. L. W. methodology; N. K. Y. and H. W. K. writing-original draft; Y. L. T., W. C., D. S., X.-Y. L., D. Y. H., H. W. K., and N. L. W. writing-review and editing; V. P., R. H., and N. L. W. resources; H. W. K. and N. L. W. project administration; N. L. W. funding acquisition.

References

1. Hood, R. L. (1982) Relationships among growth, adipose cell size, and lipid metabolism in ruminant adipose tissue. *Fed. Proc.* **41,** 2555–2561 Medline
2. Huang, Z. H., Minshall, R. D., and Mazzone, T. (2009) Mechanism for endogenously expressed Apoe modulation of adipocyte very low density lipoprotein metabolism role in endocytic and lipase-mediated metabolic pathways. *J. Biol. Chem.* **284,** 31512–31522 CrossRef Medline
3. Huang, Z. H., Reardon, C. A., Getz, G. S., Maeda, N., and Mazzone, T. (2015) Selective suppression of adipose tissue apoE expression impacts systemic metabolic phenotype and adipose tissue inflammation. *J. Lipid Res.* **56,** 215–226 CrossRef Medline
4. Gao, J., Katagiri, H., Ishigaki, Y., Yamada, T., Ogihara, T., Imai, J., Uno, K., Hasegawa, Y., Kanzaki, M., Yamamoto, T. T., Ishibashi, S., and Oka, Y. (2007) Involvement of apolipoprotein E in excess fat accumulation and insulin resistance. *Diabetes* **56,** 24–33 CrossRef Medline
5. Wang, L., Jin, Q., Lee, J. E., Su, I. H., and Ge, K. (2010) Histone H3K27 methyltransferase Ezh2 represses Wnt genes to facilitate adipogenesis. *Proc. Natl. Acad. Sci. U.S.A.* **107,** 7317–7322 CrossRef Medline
6. Yi, S. A., Um, S. H., Lee, J., Yoo, J. H., Bang, S. Y., Park, E. K., Lee, M. G., Nam, K. H., Jeon, Y. J., Park, J. W., You, J. S., Lee, S. J., Bae, G. U., Rhie, J. W., Kozma, S. C., *et al.* (2016) S6k1 phosphorylation of h2b mediates ezh2 trimethylation of h3: a determinant of early adipogenesis. *Mol. cell* **62,** 443–452 CrossRef Medline
7. Hemming, S., Cakouros, D., Isenmann, S., Cooper, L., Menicanin, D., Zannettino, A., and Gronthos, S. (2014) Ezh2 and kdm6a act as an epigenetic switch to regulate mesenchymal stem cell lineage specification. *Stem Cells* **32,** 802–815 CrossRef Medline
8. Jing, H., Liao, L., An, Y., Su, X., Liu, S., Shuai, Y., Zhang, X., and Jin, Y. (2016) Suppression of Ezh2 prevents the shift of osteoporotic MSC fate to adipocyte and enhances bone formation during osteoporosis. *Mol. Ther.* **24,** 217–229 CrossRef Medline
9. Chen, Y. H., Chung, C. C., Liu, Y. C., Yeh, S. P., Hsu, J. L., Hung, M. C., Su, H. L., and Li, L. Y. (2016) Enhancer of zeste homolog 2 and histone deacetylase 9c regulate age-dependent mesenchymal stem cell differentiation into osteoblasts and adipocytes. *Stem Cells* **34,** 2183–2193 CrossRef Medline
10. Vaswani, R. G., Gehling, V. S., Dakin, L. A., Cook, A. S., Nasveschuk, C. G., Duplessis, M., Iyer, P., Balasubramanian, S., Zhao, F., Good, A. C., Campbell, R., Lee, C., Cantone, N., Cummings, R. T., Normant, E., *et al.* (2016) Identification of (*R*)-*N*-((4-methoxy-6-methyl-2-oxo-1, 2-dihydropyridin-3-yl) methyl)-2-methyl-1-(1-(1-(2, 2, 2-trifluoroethyl) piperidin-4-yl-)ethyl)-1H-indole-3-carboxamide (CPI-1205), a potent and selective inhibitor of histone methyltransferase EZH2, suitable for phase I clinical trials for B-cell lymphomas. *J. Med. Chem.* **59,** 9928–9941 CrossRef Medline
11. Knutson, S. K., Kawano, S., Minoshima, Y., Warholic, N. M., Huang, K. C., Xiao, Y., Kadowaki, T., Uesugi, M., Kuznetsov, G., Kumar, N., Wigle, T. J., Klaus, C. R., Allain, C. J., Raimondi, A., Waters, N. J., *et al.* (2014) Selective inhibition of EZH2 by EPZ-6438 leads to potent antitumor activity in EZH2-mutant non-Hodgkin lymphoma. *Mol. Cancer Ther.* **13,** 842–854 CrossRef Medline
12. McCabe, M. T., Ott, H. M., Ganji, G., Korenchuk, S., Thompson, C., Van Aller, G. S., Liu, Y., Graves, A. P., Della Pietra, A., 3rd, Diaz, E., LaFrance, L. V., Mellinger, M., Duquenne, C., Tian, X., Kruger *et al.* (2012) EZH2 inhibition as a therapeutic strategy for lymphoma with EZH2-activating mutations. *Nature* **492,** 108–112 CrossRef Medline
13. Victora, G. D., and Nussenzweig, M. C. (2012) Germinal centers. *Annu. Rev. Immunol.* **30,** 429–457 CrossRef Medline
14. Vella, S., Gnani, D., Crudele, A., Ceccarelli, S., De Stefanis, C., Gaspari, S., Nobili, V., Locatelli, F., Marquez, V. E., Rota, R., and Alisi, A. (2013) Ezh2 down-regulation exacerbates lipid accumulation and inflammation in *in vitro* and *in vivo* NAFLD. *Int. J. Mol. Sci.* **14,** 24154–24168 CrossRef Medline
15. Hayden, A., Johnson, P. W., Packham, G., and Crabb, S. J. (2011) *S*-Adenosylhomocysteine hydrolase inhibition by 3-deazaneplanocin A analogues induces anti-cancer effects in breast cancer cell lines and synergy with both histone deacetylase and HER2 inhibition. *Breast Cancer Res. Treat.* **127,** 109–119 CrossRef Medline
16. Kim, W., Bird, G. H., Neff, T., Guo, G., Kerenyi, M. A., Walensky, L. D., and Orkin, S. H. (2013) Targeted disruption of the EZH2-EED complex inhibits EZH2-dependent cancer. *Nat. Chem. Biol.* **9,** 643–650 CrossRef Medline
17. Tan, J. Z., Yan, Y., Wang, X. X., Jiang, Y., and Xu, H. E. (2014) EZH2: biology, disease, and structure-based drug discovery. *Acta Pharmacol. Sin.* **35,** 161–174 CrossRef Medline
18. Perri, A., Vizza, D., Lofaro, D., Gigliotti, P., Leone, F., Brunelli, E., Malivindi, R., De Amicis, F., Romeo, F., De Stefano, R., Papalia, T., and Bonofiglio, R. (2013) Adiponectin is expressed and secreted by renal tubular epithelial cells. *J. Nephrol.* **26,** 1049–1054 CrossRef Medline
19. Ueno, K., Iwagawa, T., Kuribayashi, H., Baba, Y., Nakauchi, H., Murakami, A., Nagasaki, M., Suzuki, Y., and Watanabe, S. (2016) Transition of differential histone H3 methylation in photoreceptors and other retinal cells during retinal differentiation. *Sci. Rep.* **6,** 29264 CrossRef Medline
20. Dudakovic, A., Camilleri, E. T., Xu, F., Riester, S. M., McGee-Lawrence, M. E., Bradley, E. W., Paradise, C. R., Lewallen, E. A., Thaler, R., Deyle, D. R., Larson, A. N., Lewallen, D. G., Dietz, A. B., Stein, G. S., Montecino, M. A., *et al.* (2015) Epigenetic control of skeletal development by the histone methyltransferase Ezh2. *J. Biol. Chem.* **290,** 27604–27617 CrossRef Medline
21. Harris, W. S., and Jacobson, T. A. (2009) Omega-3 fatty acids. In *Clinical Lipidology: A Companion to Braunwald's Heart Disease*, p. 327, Elsevier Inc.
22. Mitrou, P., Boutati, E., Lambadiari, V., Maratou, E., Komesidou, V., Papakonstantinou, A., Sidossis, L., Tountas, N., Katsilambros, N., Economopoulos, T., Raptis, S. A., and Dimitriadis, G. (2010) Rates of lipid fluxes in adipose tissue *in vivo* after a mixed meal in morbid obesity. *Int. J. Obes. (Lond.)* **34,** 770–774 CrossRef Medline
23. Wang, J., Perrard, X. D., Perrard, J. L., Mukherjee, A., Rosales, C., Chen, Y., Smith, C. W., Pownall, H. J., Ballantyne, C. M., and Wu, H. (2012) ApoE and the role of very low density lipoproteins in adipose tissue inflammation. *Atherosclerosis* **223,** 342–349 CrossRef Medline

24. Chen, Y. C., Pohl, G., Wang, T. L., Morin, P. J., Risberg, B., Kristensen, G. B., Yu, A., Davidson, B, and Shih, I.-M. (2005) Apolipoprotein E is required for cell proliferation and survival in ovarian cancer. *Cancer Res.* **65,** 331–337 Medline
25. Su, W. P., Chen, Y. T., Lai, W. W., Lin, C. C., Yan, J. J., and Su, W. C. (2011) Apolipoprotein E expression promotes lung adenocarcinoma proliferation and migration and as a potential survival marker in lung cancer. *Lung Cancer* **71,** 28–33 CrossRef Medline
26. Pang, B., Zheng, X. R., Tian, J. X., Gao, T. H., Gu, G. Y., Zhang, R., Fu, Y. B., Pang, Q., Li, X. G., and Liu, Q. (2016) Ezh2 promotes metabolic reprogramming in glioblastomas through epigenetic repression of EAF2-HIF1a signaling. *Oncotarget* **7,** 45134–45143 CrossRef Medline
27. Wang, Y., Wang, M., Wei, W., Han, D., Chen, X., Hu, Q., Yu, T., Liu, N., You, Y., and Zhang, J. (2016) Disruption of the ezh2/miRNA/β-catenin signaling suppresses aerobic glycolysis in glioma. *Oncotarget* **7,** 49450–49458 CrossRef Medline
28. Tao, T., Chen, M., Jiang, R., Guan, H., Huang, Y., Su, H., Hu, Q., Han, X., and Xiao, J. (2017) Involvement of ezh2 in aerobic glycolysis of prostate cancer through miR-181b/HK2 axis. *Oncol. Rep.* **37,** 1430–1436 CrossRef Medline
29. Shen, X., Liu, Y., Hsu, Y. J., Fujiwara, Y., Kim, J., Mao, X., Yuan, G. C., and Orkin, S. H. (2008) EZH1 mediates methylation on histone h3 lysine 27 and complements EZH2 in maintaining stem cell identity and executing pluripotency. *Mol. Cell* **32,** 491–502 CrossRef Medline
30. Neri, F., Incarnato, D., Krepelova, A., Rapelli, S., Pagnani, A., Zecchina, R., Parlato, C., and Oliviero, S. (2013) Genome-wide analysis identifies a functional association of Tet1 and Polycomb repressive complex 2 in mouse embryonic stem cells. *Genome Biol.* **14,** R91 CrossRef Medline
31. Chatterjee, T. K., Idelman, G., Blanco, V., Blomkalns, A. L., Piegore, M. G., Jr., Weintraub, D. S., Kumar, S., Rajsheker, S., Manka, D., Rudich, S. M., Tang, Y., Hui, D. Y., Bassel-Duby, R., Olson, E. N., Lingrel, J. B, *et al.* (2011) Histone deacetylase 9 is a negative regulator of adipogenic differentiation. *J. Biol. Chem.* **286,** 27836–27847 CrossRef Medline
32. Yiew, N. K. H., Chatterjee, T. K., Tang, Y. L., Pellenberg, R., Stansfield, B. K., Bagi, Z., Fulton, D. J., Stepp, D. W., Chen, W., Patel, V., Kamath, V. M., Litwin, S. E., Hui, D. Y., Rudich, S. M., Kim, H. W., and Weintraub, N. L. (2017) Novel role for Wnt inhibitor APCDD1 in adipocyte differentiation: implications for diet-induced obesity. *J. Biol. Chem.* **292,** 6312–6324 CrossRef Medline
33. Zhou, H., Black, S. M., Benson, T. W., Weintraub, N. L., and Chen, W. (2016) Berardinelli-Seip congenital lipodystrophy 2 (BSCL2)/SEIPIN is not required for brown adipogenesis but regulates brown adipose tissue development and function. *Mol. Cell Biol.* **36,** 2027–2038 CrossRef Medline
34. Kuhel, D. G., Konaniah, E. S., Basford, J. E., McVey, C., Goodin, C. T., Chatterjee, T. K., Weintraub, N. L., and Hui, D. Y. (2013) Apolipoprotein E2 accentuates postprandial inflammation and diet-induced obesity to promote hyperinsulinemia in mice. *Diabetes* **62,** 382–391 CrossRef Medline
35. Galarraga, M., Campión, J., Muñoz-Barrutia, A., Boqué, N., Moreno, H., Martínez, J. A., Milagro, F., and Ortiz-de-Solórzano, C. (2012) Adiposoft: automated software for the analysis of white adipose tissue cellularity in histological sections. *J. Lipid Res.* **53,** 2791–2796 CrossRef Medline
36. Benson, T. W., Weintraub, D. S., Crowe, M., Yiew, N. K. H., Popoola, O., Pillai, A., Joseph, J., Archer, K., Greenway, C., Chatterjee, T. K., Mintz, J., Stepp, D. W., Stansfield, B. K., Chen, W., Brittain, J., *et al.* (2018) Deletion of the Duffy antigen receptor for chemokines (DARC) promotes insulin resistance and adipose tissue inflammation during high fat feeding. *Mol. Cell Endocrinol.* **473,** 79–88 CrossRef Medline